Targeted Nanogel Conjugate for Improved Stability and Cellular Permeability of Curcumin: Synthesis, Pharmacokinetics, and Tumor Growth Inhibition

Xin Wei, Thulani H. Senanayake, Anna Bohling, and Serguei V. Vinogradov*

Department of Pharmaceutical Sciences and Center for Drug Delivery and Nanomedicine, College of Pharmacy, University of Nebraska Medical Center, Omaha, Nebraska 68198, United States

 S *Supporting Information*

ABSTRACT: Curcumin (CUR) is a unique natural compound with promising anticancer and anti-inflammatory activities. However, the therapeutic efficacy of curcumin was challenged in clinical trials, mostly due to its low bioavailability, rapid metabolism, and elimination. We designed a nanodrug form of curcumin, which makes it stable and substantially enhances cellular permeability and anticancer activity at standard oral administration. Curcumin was conjugated as an ester to cholesteryl-hyaluronic acid (CHA) nanogel that is capable of targeted delivery to CD44-expressing drug-resistant cancer cells. CHA-CUR nanogels demonstrated excellent solubility and sustained drug release in physiological conditions. It induced apoptosis in cancer cells, suppressing the expression of NF-κB, TNF-α, and COX-2 cellular targets similar to free curcumin. Pharmacokinetic/pharmacodynamic (PK/PD) studies also revealed improved circulation parameters of CHA-CUR at oral, *i.p.* and *i.v.* administration routes. CHA-CUR

showed targeted tumor accumulation and effective tumor growth inhibition in human pancreatic adenocarcinoma MiaPaCa-2 and aggressive orthotropic murine mammary carcinoma 4T1 animal models. CHA-CUR treatment was well-tolerated and resulted in up to 13-fold tumor suppression, making this nanodrug a potential candidate for cancer prevention and therapeutic treatment.

KEYWORDS: *Curcumin, nanogel−drug conjugate, NF-κB inhibition, PK/PD parameters, animal cancer models*
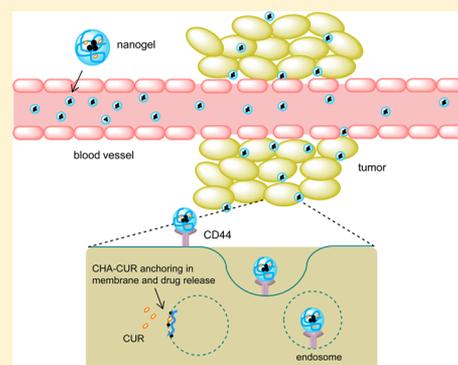
■ INTRODUCTION

Curcumin (CUR) is a natural polyphenol extracted from turmeric, an Eastern spice, which demonstrated a spectrum of biological activities, including antioxidant, anti-inflammatory, and anticancer activities.[1−4] Anticancer activities of curcumin included blockade of cellular targets, which are responsible for cancer initiation, growth, and metastasis.[5] It was especially effective in the inhibition of nuclear factor-kappa B (NF-κB), an important cellular transcription regulator, which switches multiple downstream signaling pathways and gene activities.[4−10] Curcumin reportedly suppressed colorectal cancer growth in animal model by inhibition of NF-κB/PI3K/Src pathway,[8] and in breast cancer models (MDA-MB-231 and BT-483) by inhibition of NF-κB, cyclin D1, and matrix metalloproteinases (MMPs).[9] Other antiapoptotic factors like cyclooxygenase-2 (COX-2), survivin, and vascular endothelial growth factor (VEGF) have been down-regulated after the treatment with curcumin via the suppression of NF-κB activity.[5,11] It sensitized tumor cells to the activity of other drugs in combination with other chemotherapeutics.[7,8,12] Curcumin was shown to reverse multidrug resistance, reducing the expression of P-glycoprotein (P-gp) in cancer cells via PI3K/NF-κB pathway.[6]

Despite the promising anticancer activity, clinical trials demonstrated low or no therapeutic effect of free oral curcumin on various types of cancer.[13] The principal factors of the failure were very low solubility, poor bioavailability, rapid inactivation caused by limited stability of free curcumin in solution, active binding with serum proteins, and fast clearance from circulation.[14] To address some of these problems, nano-encapsulation of curcumin was proposed, and currently, liposome or PLGA nanoparticles showed promising results.[15,16] However, liposome encapsulation did not enhance curcumin stability under *in vivo* conditions.[16] Stable curcumin derivatives could be obtained by modification of phenol hydroxyls, e.g., through PEGylation.[17] New potential therapeutic curcumin derivatives have been recently reviewed.[18]

Conjugation of curcumin through phenol hydroxyls with polymeric micelles was able to significantly increase its stability and allow the sustained drug release due to the cleavage of the reversible ester linkage.[19] Curcumin was also conjugated with hyaluronic acid to improve its aqueous solubility and stability.[20]

The HA-CUR conjugate could self-assemble into micelles in aqueous solution and deliver the drug to cancer cells through cleavage of the ester bond.[20] Recently, we evaluated a conjugate of curcumin with cholesteryl hyaluronic acid (CHA-CUR) in order to obtain effective nanodrug that combines the enhanced drug stability and cellular uptake with a sustained drug release and effective targeted delivery to tumors. In this study, we demonstrated that CHA-CUR had a superior stability compared to free curcumin, could be efficiently delivered in tumors via interaction with CD44 receptors overexpressed on aggressive and drug-resistant cancer cells, and demonstrated advanced pharmacokinetic (PK) characteristics *in vivo* and high tumor growth inhibition in animal cancer models.

■ MATERIALS AND METHODS

Materials. Most chemical reagents and solvents were purchased from Sigma-Aldrich (St. Louis, MO) with the highest available purity and used without purification unless otherwise indicated. Hyaluronic acid sodium salt (MW 62 kDa) was purchased from Quingao Biomedical (Chaska, China). Proton NMR spectra were recorded using a 500 MHz Varian NMR-spectrometer and tetramethylsilane as a standard. Hydrodynamic diameter, polydispersity, and zeta potential were measured by Zetasizer Nano-ZS90 (Malvern Instruments, Southborough, MA). UV absorbance was measured by Biophotometer (Eppendorf, Hamburg, Germany) or Nano-Drop 2000 spectrophotometer (Thermo Fisher Scientific, Waltham, MA).

Cells. Murine mammary carcinoma cell line 4T1 (a kind gift from Dr. Joseph Vetro, UNMC) and human pancreatic adenocarcinoma cells MiaPaCa-2 (a kind gift from Dr. Surinder Batra, UNMC) were maintained in Dulbecco's modified Eagle's medium (DMEM, HyClone/ThermoScientific) supplemented with 10% fetal bovine serum (FBS), 1% L-glutamate, and 2% penicillin/streptomycin. All cells were cultured at 37 °C in humidified atmosphere with 5% CO_2.

Synthesis. CHA-CUR was synthesized using a modified method.[21] Cholesteryl-amine linker was synthesized by reacting cholesteryl chloroformate (3.36 g, 0.75 mmol) with 2,2′-(ethylenedioxy)-bis-ethylamine (5g, 30 mmol) in 20 mL of dichloromethane for 24 h. The product was isolated by column chromatography on silicagel using a stepwise methanol-dichloromethane gradient. Sodium salt of HA was converted into H+ form by the treatment with Dowex-50 (H+). CHA with six cholesterol moieties per HA molecule was synthesized by modification of HA (6 g, 15 mmol carboxyl groups) dissolved in 100 mL of DMSO/water (7:3 v/v) with cholesteryl-amine linker (576 mg, 0.96 mmol) in the presence of 150 mg (0.96 mmol) of 1-ethyl-3-(3-(dimethylamino)-propyl) carbodiimide (EDC) and 135 mg (0.96 mmol) of hydroxybenzotriazole (HOBT) for 48 h at 25 °C. The product was isolated by dialysis (MWCO 12−14 kDa) against water (3×, 24 h) and concentrated *in vacuo*. The CHA-CUR conjugate was synthesized by adding curcumin (1.5 g, 4 mmol) in 5 mL of DMSO to the solution of CHA (5g), EDC (0.77g, 4 mmol), and DMAP (122 mg, 1 mmol) in 100 mL of DMSO/water (7:3 v/v). The reaction mixture was stirred for 3 days under argon, and the CHA-CUR conjugate was purified by dialysis (MWCO 12−14 kDa) against water (3×, 24 h) at 4 °C. An average yield was 85%. The curcumin content in the lyophilized product was calculated from ¹H NMR spectrum recorded in *d*-DMSO.

Amino-CHA and amino-CHA-CUR were obtained by direct modification of 2% of carboxyl groups in the presence of EDC/HOBT in DMSO/water (7:3 v/v) with 5-fold excess of 2,2′-(ethylenedioxy)-bis-ethylamine. The modified amino-polymers were dialyzed (MWCO 12−14 kDa) against water (3×, 24 h) at 4 °C and lyophilized. Tritium-labeled or Rhodamine-labeled CHA-CUR were synthesized by conjugation of the amino-polymers with [³H]-succinimidyl propionate (110 μCi/mmol, Moravek Biochemicals, CA, USA) or Rhodamine isothiocyanate, respectively, in DMSO/water (7:3 v/v) for 2 h at 25 °C. The labeled CHA or CHA-CUR conjugates were isolated on NAP-10 column and lyophilized.

Nanogel particles have been produced by sonication of aqueous solutions of CHA or CHA-CUR for 30 min and characterized by hydrodynamic diameter, polydispersity, and zeta-potential measured using dynamic light scattering.

Cellular Uptake. MiaPaCa-2 cells were seeded in 24-wells plates. Rhodamine-labeled HA and CHA nanogel (50 μg/mL; cholesterol contents 6, 10, and 18 moieties per polymer molecule) were incubated with cells in full medium for 2 h at 4 or 37 °C in triplicates. Cells were collected, washed 3 times with ice cold PBS, and treated with cell lysis buffer (100 μL) for 10 min. Each sample was transferred into black-walled plate, and fluorescence was measured using a BioTek FLx-800 fluorescent reader.

To investigate the uptake pathways for CHA nanogels, we used endocytosis pathway inhibitors.[22] Uptake of Rh-CHA in MiaPaCa-2 cells was measured after pretreatment with free HA (2 mg/mL) to block CD44 receptors, using low temperature (4 °C) to inhibit endocytosis, in the presence of 10 μg/mL chlorpromazine (clathrin-dependent endocytosis inhibitor), 10 μg/mL genistein (caveolae-dependent endocytosis inhibitor), or 100 μg/mL amiloride (macropinocytosis inhibitor). The internalized nanogels were quantified by fluorescence using calibration curves.

Drug Release. Release of free curcumin from CHA-CUR under physiological and gastrointestinal conditions was studied in simulated gastric fluid (SGF) and simulated intestinal fluid (SIF), respectively, as earlier described.[23] Briefly, SGF was prepared by dissolving 3.2 g/L of pepsin from porcine stomach mucosa in 34 mM sodium chloride and 84 mM hydrochloric acid solution. The final pH of SGF was adjusted to 1.2. SIF was prepared by dissolving 10 g/L of pancreatin in 50 mM of monobasic potassium phosphate and 15 mM sodium hydroxide solution. The final pH of SIF was adjusted to 6.8. CHA-CUR solution (20 mg/mL, 0.1 mL) was mixed with 2.9 mL of SGF or SIF and incubated at 37 °C. At the preset time points (0.5, 1, 2, 4, 8, 24, and 48 h), 0.25 mL aliquots were withdrawn and filtered using Amicon Ultra 0.5 centrifugal filter (MWCO 3 kDa). UV absorbance of curcumin was measured in filtrates at 420 nm and corrected by SGF or SIF absorbance. The curcumin standard curve at serial dilutions was used in calculations, and data were expressed as cumulative drug release at different time points.

Cytotoxicity. The cytotoxicity of CHA-CUR conjugate was compared with curcumin dissolved in DMSO in two cancer cell lines, murine mammary carcinoma 4T1 cells and human pancreatic adenocarcinoma MiaPaCa-2 cells, using standard MTT assay. Briefly, cell suspensions were seeded in 96-well plates at a density of 5000 cells/well, and cells were allowed to attach overnight at 37 °C. Serial dilutions of sample solutions in full medium were added into wells, and cells were incubated for 72 h at 37 °C. Metabolic activity of cells was determined by

incubation with 20 μL per well of MTT solution (5 mg/mL) in sterile PBS for 4 h at 37 °C. Then, 150 μL of DMSO was added to each well to dissolve the formed blue formazan, and optical absorbance was measured at 570 nm using a Model 680 microplate reader (BioRad, Hercules, CA). The cytotoxicity was expressed as the percentage of surviving cells compared to untreated cells at different curcumin and CHA-CUR concentrations, and the concentrations of 50% cell survival (IC_{50} values) were calculated using a trapezoid rule.

Apoptosis Assay. 4T1 cells were seeded in 6-well plates and allowed to attach overnight. Curcumin or CHA-CUR were used at equal drug concentrations, 5, 10, 15, and 20 μg/mL, to treat cells for 48 h. Annexin V-FITC apoptosis detection kit (Sigma-Aldrich, St-Louis, MO) was applied to analyze the degree of apoptosis in treated cells according to manufacturer's protocol. The amount of apoptotic cells in each sample was quantified by flow cytometry.

Real-Time RT-PCR. 4T1 cells were seeded in 6-well plates and allowed to attach overnight. Ten micromolar curcumin or CHA-CUR (by drug content) were used to treat cells for 24 and 48 h. RNA was extracted from treated cells using a Trizol reagent (1 mL of Trizol per million cells). Half of a milliliter of chloroform per 1 mL of Trizol was added to remove proteins. After centrifugation (12,000g, 15 min at 4 °C), RNA from the supernatant was precipitated in isopropyl alcohol (10 min, 25 °C) and centrifuged. The RNA pellet was washed with 75% ethanol, dried on air, and redissolved in RNase-free water. RNA content was quantified by UV absorbance at 260 nm. Real-time RT-PCR analysis was performed on BioRad iQ5 thermocycler using iScript One-Step RT-PCR kit with SYBR Green (BioRad, USA). GAPDH, NF-κB, TNF-α, and COX-2 optimized primer pairs were obtained from Qiagen (USA). Crossing threshold values for individual genes were normalized to GAPDH. RNA expression level was expressed as a fold change relative to the nontreated control.

In Vivo Biodistribution. Animal studies were performed according to the principles of animal care outlined by the National Institutes of Health, and protocols were approved by the Institutional Animal Care and Use Committee at University of Nebraska Medical Center. Female Balb/c and nu/nu mice (age 6–8 weeks) used in experiments were purchased from Charles River Laboratories (Wilmington, MA) and maintained under sterile conditions in controlled environment.

For bioimaging experiment, human pancreatic adenocarcinoma MiaPaCa-2 cells were resuspended in the serum-free medium containing 20% Matrigel (Becton-Dickinson, San Diego, CA), and 5×10^6 cells were injected subcutaneously into the right flank of each mouse. When the tumor size exceeded 50 mm^3, each mouse was injected intravenously with 200 μL of Rhodamine-labeled CHA-CUR solution (2 mg/mL). Ninety-six hours after injection, mice were sacrificed and systemically perfused with PBS. Major organs including brain, heart, lung, liver, spleen, kidney, and tumor were collected, and their fluorescent images were obtained using Xenogen IVIS-200 bioimager. The fluorescence intensity in organs was quantitatively calculated by Live Image 2.50 software program. Results have been expressed as a fluorescence density (fluorescent intensity per image pixel).

Pharmacokinetic Study. Half of a milligram of ^{3}H-labeled CHA-CUR was given to each Balb/c mouse by i.v. injection, i.p. injection, or oral gavage (groups, n = 3). At predetermined time points (0.5, 1, 2, 8, and 24 h), mice were sacrificed, and blood and major organs including heart, lung, liver, spleen, and kidney

have been collected. The blood was centrifuged to get plasma (2500g, 10 min at 4 °C). The collected tissues were homogenized with Solvable (Packard Bioscience, USA) according to manufacturer's instruction. Plasma and tissue homogenates were treated with methanol for 10 min to extract CHA-CUR, and then centrifuged (2500g, 5 min). The supernatants were dried and dissolved in Ultima Gold (Sigma) scintillator cocktail, and tritium radioactivity was analyzed using a Packard liquid scintillation counter. Major organs have been analyzed 24 h postinjection in order to determine biodistribution of CHA-CUR at different administration routes.

Plasma kinetic parameters of CHA-CUR were calculated from drug concentration–time curve. The maximum plasma concentration (C_{max}) and the time to reach C_{max} (t_{max}) were obtained directly from the drug concentration–time data. The area under the concentration–time curve (AUC) was used as a measure of total amount of CHA-CUR that reached systemic circulation. AUC from time zero to the last sampling time (AUC_{0-t}) was calculated by the trapezoid rule. The elimination rate constant, k_{el}, was obtained from the slope of the drug concentration–time curve. The elimination half-life ($t_{1/2}$) was calculated as 0.693 divided by k_{el}. The mean residence time (MRT) was estimated from AUMC/AUC, where AUMC is the area under the first moment curve. Drug clearance (CL) is the volume of plasma in the vascular compartment cleared of drug per unit time.

Tumor Growth Inhibition. Human pancreatic adenocarcinoma MiaPaCa-2 xenograft model was established in female nu-nu mice. Cancer cells (5×10^6 cells) were injected subcutaneously in the right flank of each mouse in serum-free medium containing 20% Matrigel. Mice were divided on the 10th day after tumor inoculation into three treatment groups: control, curcumin/DMSO, and CHA-CUR/saline (n = 8). The treatment by i.p. injection of 6 mg/kg curcumin or equivalent amount of CHA-CUR (by drug content) was performed twice every week. The control group received i.p. injections of normal saline. Animals have been monitored daily from Day 10. Tumor volume was measured by digital calipers and calculated using the equation: $V = L/2 \times W^2$, where L and W are length and width of tumor (mm).

Orthotopic murine mammary 4T1 tumor model was established in female Balb/c mice. 4T1 cells (0.5×10^6) were resuspended in serum-free medium containing 20% Matrigel and injected subcutaneously in the lower abdominal mammary pad of each Balb/c mouse. Mice were randomly divided into 3 groups (n = 8). The treatment with CUR/DMSO and CHA-CUR/saline was started the next day after tumor inoculation and continued every other day. In curcumin group, 0.28 mg of CUR dissolved in 60% DMSO was administered per mouse, and in CHA-CUR group, 4 mg of CHA-CUR (7% CUR content) dissolved in water was administered per mouse by oral gavage. In control group, mice received water. Animals have been monitored daily during treatment, and tumor volume was calculated as described above.

Statistical Analysis. Statistical analysis was performed by application of the two-tailed unpaired Student's t test using SPSS 16.0 software. Differences between groups were considered significant at $P < 0.05$.

■ RESULTS

Synthesis and Characterization of CHA-CUR Nanogel. We simplified the synthesis of CHA-CUR to make it using
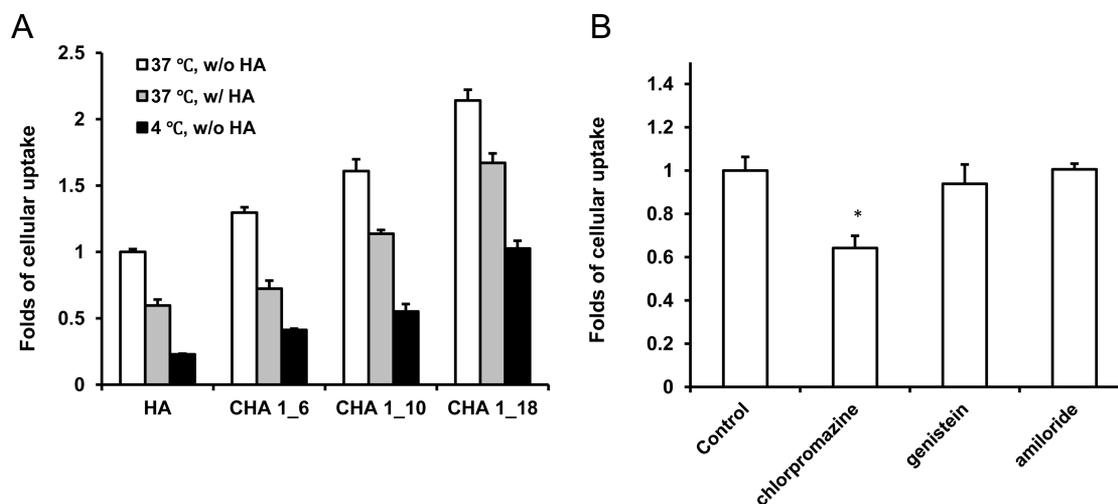
Figure 1. Cellular uptake studies in MiaPaCa-2 cells. (A) Cellular uptake of HA and CHA with different cholesterol content. CHA 1_6, CHA 1_10, and CHA 1_18 denote CHA nanogels, which contain 6, 10, or 18 cholesterol molecules per one HA molecule, respectively. HA pretreatment: 3 mg/mL, 30 min. Data were normalized to show enhancement of the cellular uptake without HA pretreatment at 37 °C. (B) Cellular uptake of CHA following pretreatment with endocytosis inhibitors: chlorpromazine (clathrin-mediated endocytosis), genistein (caveolae-mediated endocytosis), and amiloride (macropinocytosis). *, $P < 0.05$, compared to control group. Data were normalized to the cellular uptake of CHA without pretreatment with endocytosis inhibitors.
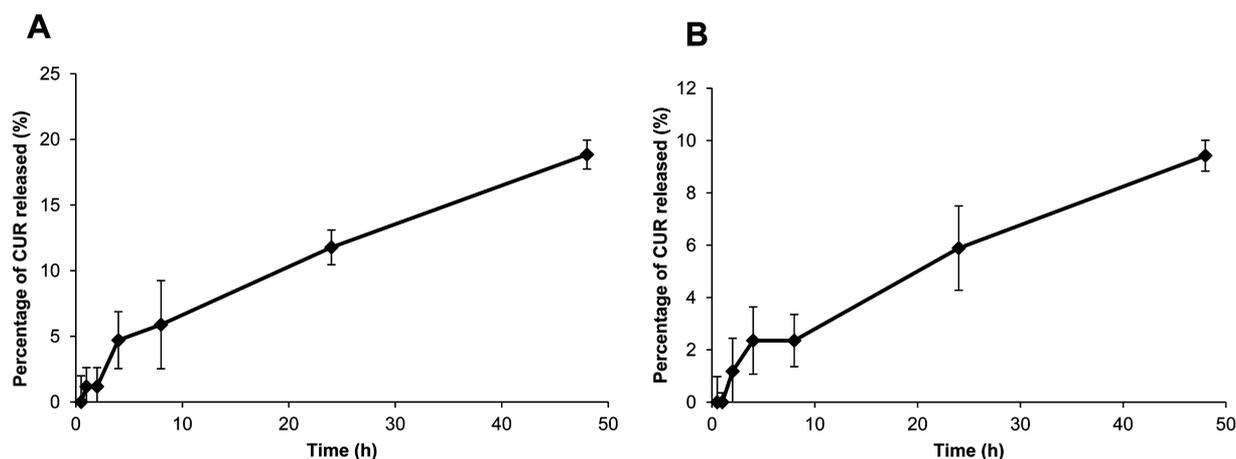

Figure 2. Drug release after incubation of CHA-CUR in (A) simulated gastric fluid (SGF), pH 1.2, and (B) simulated intestinal fluid (SIF), pH 6.8, at 37 °C. Data are expressed as a percentage of the released CUR ± SEM ($n = 5$).

cleaner chemistry with limited amount of organic solvents.[21] Required amounts of cholesterol moieties were attached to HA polymer through short linkers and amide bond formation. The optimal cholesterol content in CHA was 3−5% to ensure small particle size and good solubility. Curcumin was conjugated onto the CHA polymer via ester bond formation. The solubility of CHA-CUR in water was ca. 400-fold higher compared to free curcumin. The CHA-CUR conjugate formed uniform compact nanogel particles of 20 nm in diameter with a spherical morphology and negative surface charge after ultrasonication in aqueous solution. Scheme of the chemical synthesis and physicochemical characterization of CHA-CUR are shown in the Supporting Information.

Cellular Uptake. The cellular uptake study was performed in MiaPaCa-2 cell culture. As shown in Figure 1, CHA nanogel mediated higher cellular internalization compared with non-modified HA polymer. Increase in cholesterol content resulted in stronger cellular uptake; however, specificity of receptor-mediated endocytosis was reduced. Twenty to forty perecent of inhibition was observed at the pretreatment with free HA to block CD44 receptors. At low temperature (4 °C), the internalization process also suppressed by 50%−80%, confirming the endocytosis mechanism of CHA nanogel uptake due to the lower cellular metabolism compared to 37 °C. In the case of higher cholesterol content, the effect was lower, signaling direct membrane-specific interaction of CHA nanogels. We determined the specific internalization pathways of CHA nanogels using the commercial inhibitors, chlorpromazine, genistein, and amiloride, in order to suppress clathrin-mediated endocytosis, caveolae-mediated endocytosis, and macropinocytosis, respectively.[22] Following genistein and amiloride pretreatment, no changes in cellular uptake were observed; meanwhile, there was significant lower cellular uptake after chlorpromazine pretreatment. These results indicated that the clathrin-dependent endocytosis is the major uptake pathway for CHA nanogel via CD44 receptor-mediated internalization at the low (3−5%) content of cholesterol. CHA uptake mechanisms do not involve caveolae-dependent endocytosis or macropinocytosis.

Gastrointestinal Stability. Stability of CHA-CUR in GI tract is an important factor at oral administration. Therapeutic
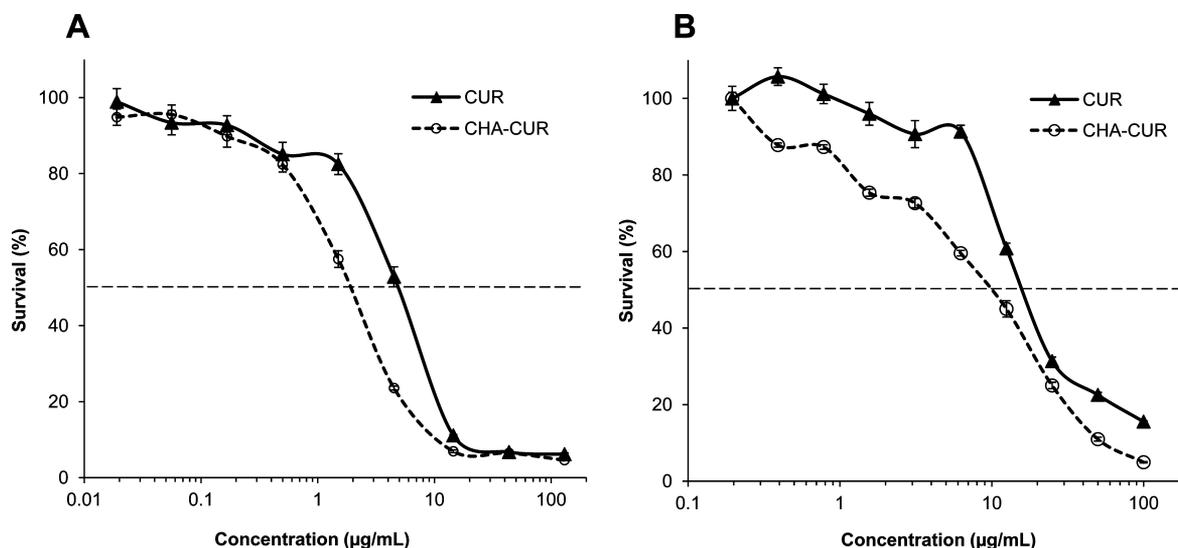
Figure 3. Cytotoxicity of CHA-CUR compared to free curcumin in (A) 4T1 and (B) MiaPaCa-2 cells (MTT assay, 72 h, 37 °C). Data are shown as means ± SEM ($n = 8$).

efficacy of CHA-CUR depends on the release/inactivation of curcumin in GI tract and the penetration of intact CHA-CUR into the blood. We tested drug release from CHA-CUR in SGF at pH 1.2 (stomach conditions) and SIF at pH 6.8 (small intestine conditions) to evaluate linker stability at specific pHs and in the presence of proteolytic enzymes. The transit time in stomach and intestine is generally 4 and 8 h, respectively. As shown in Figure 2, during 4 h incubation in SGF, only 5% of free curcumin was released from CHA-CUR conjugate. Likewise, less than 3% of CUR was cleaved from CHA-CUR after 8 h of incubation in SIF. Maximal drug release after 48 h of incubation was less than 20 and 10% in SGF and SIF, respectively. This result demonstrates that most CHA-CUR can be absorbed in GI tract and enter blood circulation in the form of active conjugate due to its high solubility and stability in GI condition. Oral administration may result in the loss of 2−5% of the conjugated curcumin.

Cytotoxicity and Apoptosis Studies. The cytotoxicity of CHA-CUR was compared to free curcumin in human pancreatic cancer MiaPaCa-2 cells and murine mammary cancer 4T1 cells, which were used in tumor growth inhibition studies in cancer mouse models. In the thiazolyl blue (MTT) cytotoxicity assay, CHA-CUR showed a significant 2.5-fold higher efficacy in 4T1 cells (IC$_{50}$, 2 vs 5 μg/mL) and 2-fold higher efficacy in MiaPaCa-2 cells (IC$_{50}$, 9 vs 18 μg/mL) compared to curcumin (Figure 3).

Apoptosis was examined in 4T1 cells treated by CHA-CUR and curcumin using Annexin V-FITC/propidium iodide assay and flow cytometry (Table 1). The numbers of apoptotic cells increased dose-dependently in both groups. CHA-CUR confirmed its higher efficacy against cancer cells by inducing 2 times higher apoptosis compared to free curcumin in the drug concentration range of 10−15 μg/mL. These results are consistent with our MTT data that CHA-CUR is a more effective anticancer drug.

Effect on Cellular Targets. Curcumin can target various molecular mechanisms, but TNF-α, NF-κB, and COX-2 are the most important cellular targets affected in cancer treatment. We examined expression of these genes in 4T1 cells treated with CHA-CUR using a quantitative real-time RT-PCR. The expression of TNF-α and NF-κB mRNAs was significantly

**Table 1. Apoptosis in 4T1 Cells after CUR and CHA-CUR Treatment**[a]

sample	apoptotic cells (%)
CUR, 5 μg/mL	6.89
CUR, 10 μg/mL	11.15
CUR, 15 μg/mL	17.01
CUR, 20 μg/mL	33.9
CHA-CUR, 5 μg/mL	6.09
CHA-CUR, 10 μg/mL	25.04
CHA-CUR, 15 μg/mL	36.75
CHA-CUR, 20 μg/mL	45.2

[a]Annexin V-FITC kit (Sigma-Aldrich, USA) was used for flow cytometry analysis. Cells were treated for 48 h.

inhibited with either curcumin or CHA-CUR (90% inhibition after 24−48 h treatment) (Figure 4). We also observed a statistically significant down-regulation of COX-2 expression in curcumin and CHA-CUR groups. The mRNA expression was reduced stronger in CHA-CUR group treated for 48 h, probably, due to the sustained drug release and stability. Altogether, CHA-CUR caused apoptosis and cytotoxicity in cancer cells by suppressing the same cellular targets (NF-κB, TNF-α, and COX-2) as the free curcumin.

***In Vivo* Biodistribution.** The tumor-targeting ability and *in vivo* organ distribution of CHA-CUR have been measured using an *ex vivo* fluorescent bioimaging (Figure 5). Rhodamine-labeled CHA-CUR was injected intravenously into tumor-bearing mice, and fluorescence of tumors and organs were analyzed using IVIS-200 imaging system. The highest fluorescence density was observed in liver (high content of CD44 receptors) and tumors compared to other organs. Interestingly, the accumulation in tumors was significantly higher than in kidneys ($p < 0.05$). Even 96 h after injection, there was still a high amount of CHA-CUR in tumor and liver. Our results indicated that CHA-CUR can be retained and slowly cleared from the body.

Pharmacokinetic Study. Plasma pharmacokinetics and organ biodistribution of ^{3}H-labeled CHA-CUR was evaluated after single intravenous, intraperitoneal, or oral (25 mg/kg) administration in mice. Plasma samples were analyzed at preset
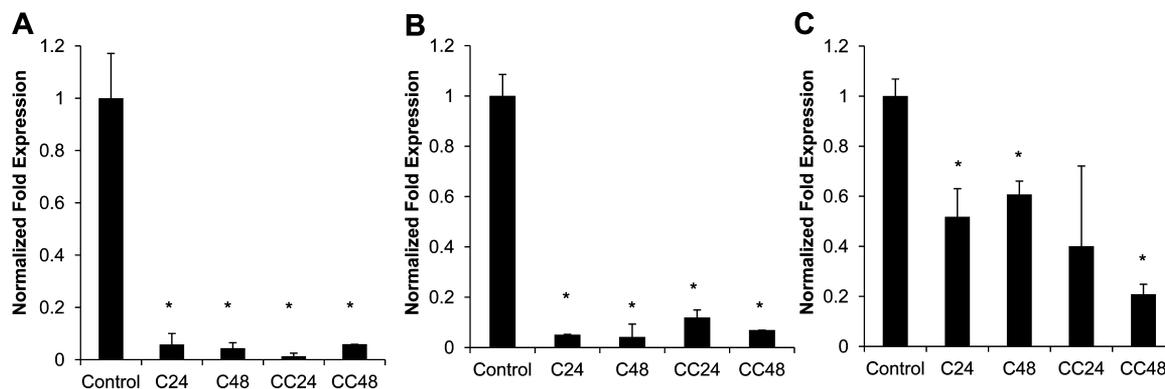
Figure 4. Level of mRNA expression of (A) NF-κB, (B) TNF-α, and (C) COX-2 after the treatment of 4T1 cells by curcumin or CHA-CUR measured by quantitative real-time RT-PCR. Crossing threshold values for individual genes were normalized to GAPDH cellular control. Changes in mRNA expression were expressed as fold change relative to the control. C24/C48, cells treated with CUR for 24 or 48 h; CC24/CC48, cells treated with CHA-CUR for 24 or 48 h. Data are shown as means $\pm$ SD; *, $P < 0.05$, compared to control.
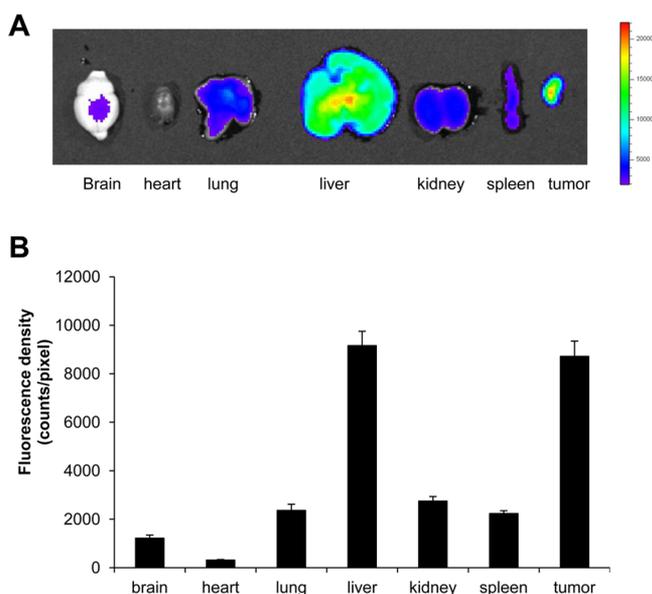
Figure 5. *Ex vivo* fluorescent imaging 4 days after *i.v.* injection of Rhodamine-labeled CHA-CUR in MiaPaCa-2 xenograft model. (A) Fluorescence images of excised organs and tumors. (B) Fluorescence density in each organ. Values indicate fluorescence counts per pixel. Data were expressed as mean $\pm$ SEM ($n = 3$).

time points, and the CHA-CUR concentration was determined from calibration curve and then recalculated to obtain curcumin concentration using an assumption that the loss of curcumin from CHA-CUR was less than 5% during the 24 h testing period. As shown in Figure 6A, after CHA-CUR administration, plasma concentration of curcumin increased gradually within 1 h (*i.p.* C_{max}, 1.8 μg/mL; oral C_{max}, 0.85 μg/mL), then declined to 0.3−0.46 μg/mL within 8 h, and remained mostly constant up to 24 h. The calculated pharmacokinetic/pharmacodynamic (PK/PD) parameters are shown in Table 2. These data have been compared with the reported data for free curcumin.[24] The comparison showed that it takes less time to reach C_{max} at oral administration of CHA-CUR. Similarly, half-life ($t_{1/2}$) of CHA-CUR was much longer, showing over 20-fold increase at *i.v.* and oral administrations compared to free curcumin. Likewise, CHA-CUR had a longer half-life than liposomal curcumin (14-fold for *i.v.* and 6-fold for oral administration), as well as up to 10-fold longer MRT (8.51 vs 0.81 h for *i.v.*; 8.95 vs 5.58 h for

oral).[25] Increased plasma concentration is a clear indication of the faster absorption of CHA-CUR from GI tract and the lower clearance from circulation compared to liposomal curcumin. Furthermore, we observed higher $t_{1/2}$, t_{max}, and MRT values similar to *i.v.* and *p.o.* when CHA-CUR administer in *i.p.* route of administration (Table 2). Also, we observed the significant increase in AUC values for CHA-CUR compared to free curcumin (7.7−12.2 vs 0.44−3.6 h μg/mL) obtained even at 6−285-fold higher doses than in our study. Comparing three routes of administrations, we observed longer maximum clearance time when CHA-CUR was administered orally compared to *i.v.* and *i.p.* routes (3.1 vs 2 h).

The organ distribution of CHA-CUR was monitored 24 h post *i.v.*, *i.p.*, and oral administration in mice. As shown in Figure 6B, liver was the major organ accumulating CHA-CUR, as is consistent with high CD44 expression level. A major drug excretion in organ and kidney accumulated low amounts of CHA-CUR. These results are consistent with our *ex vivo* imaging results about CHA-CUR accumulation.

Tumor Growth Inhibition. To evaluate therapeutic efficacy of CHA-CUR, we studied tumor growth inhibition in human pancreatic MiaPaCa-2 xenograft and murine mammary 4T1 orthotopic cancer models (Figure 7). In MiaPaCa-2 model, mice were treated by *i.p.* injections of curcumin/DMSO or CHA-CUR/saline. Statistically significant tumor growth inhibition was observed between control and CHA-CUR groups ($P < 0.05$) and curcumin and CHA-CUR groups ($P < 0.05$). The CHA-CUR treatment resulted in 15-fold and 5-fold decrease in the mean tumor volume on Day 49 compared to control group and free curcumin group, respectively.

In 4T1 orthotopic model, mice were treated with curcumin/DMSO solution or CHA-CUR/water through oral gavage (0.28 mg CUR per mouse). We observed a significant difference in tumor growth between control group and CHA-CUR group ($P < 0.05$) and between curcumin group and CHA-CUR group from Day 26 ($P < 0.05$). Tumor volume in CHA-CUR group on Day 28 was 2.5-fold smaller that in the control group. Two mice from the control group and one mouse from the curcumin-treated group died in the result of development of very aggressive and metastatic tumor. No significant weight loss associated with the systemic toxicity was observed in animals treated with curcumin or CHA-CUR.

On the basis of our data, *i.p.* and orally administered CHA-CUR rapidly goes into blood circulation and reaches tumor
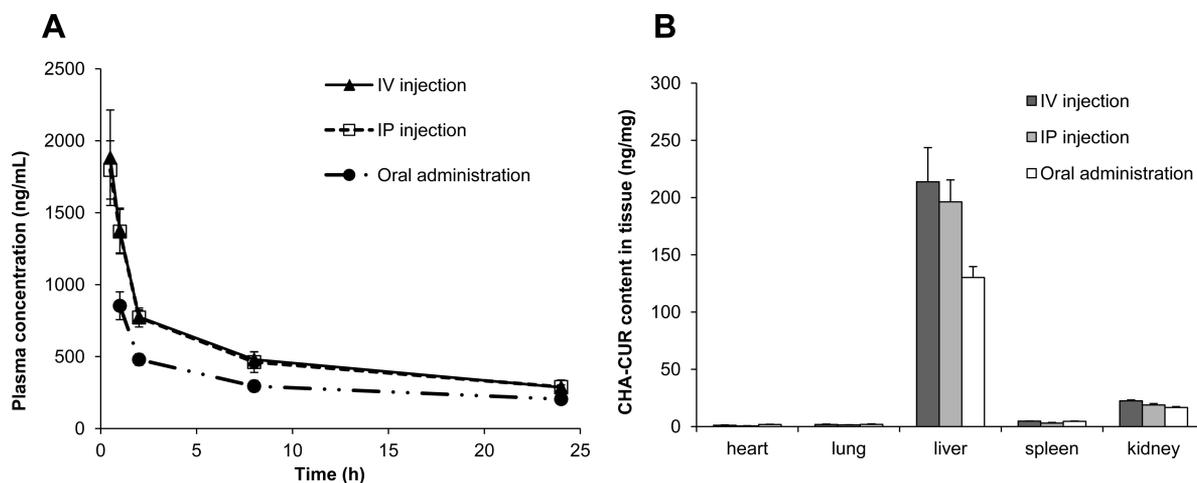
Figure 6. Pharmacokinetic and organ distribution studies. (A) Plasma concentration–time curve obtained after administration of 0.5 mg (^{3}H) CHA-CUR by *i.v.*, *i.p.*, and *p.o.* routes. (B) Organ biodistribution of (^{3}H) CHA-CUR in mice 24 h after *i.v.*, *i.p.*, and oral administration. Data were expressed as mean ± SEM (n = 3).

Table 2. Pharmacokinetic Parameters of (^{3}H) CHA-CUR (Dose, 25 mg/kg) in Mice (Weight, 20 g)^a

	curcumin		
parameters	*i.v.*	*i.p.*	*p.o.*
dose (mg kg)	1.75	1.75	1.75
C_0 (ng/mL)	11620		
C_{max} (ng/mL)		1871 ± 329	853 ± 96
t_{max} (h)		0.5	1.0
$t_{1/2}$ (h)	21.23 ± 0.16	24.07 ± 7.67	23.40 ± 7.46
MRT (h)	8.51 ± 0.52	8.58 ± 0.62	8.95 ± 0.51
$AUC_{0-\tau}$ (h·ng/mL)	12252 ± 770	12059 ± 838	7781 ± 449
$AUC_{0-\infty}$ (h·ng/mL)	16830 ± 1111	16686 ± 1018	11053 ± 843
CL (mL/h)	2.08 ± 0.14	2.10 ± 0.13	3.17 ± 0.24

^{a}Data are mean ± SD for CHA-CUR after recalculating based on CUR content of 7%. The CUR cleaved from the conjugate (<5%) was not taken into account.

sites, accumulating in cancer cells mostly through the CD44 receptor-mediated endocytosis. Effective internalization of CHA-CUR and sustained release of intact curcumin inside the cells resulted in very efficient inhibition of cancer cell growth compared to free drug, which has a poor bioavailability and is effectively inactivated *in vivo*, has ineffective cellular accumulation, and is rapidly cleared from blood binding serum proteins. Thus, the nanoengineered form of curcumin, CHA-CUR, represents a promising new anticancer therapeutic with additional benefits of low toxicity, targeted action, and extended activity.

■ DISCUSSION

Curcumin has already been extensively studied as an anticancer agent. Unfortunately, direct oral administration of curcumin in clinical trials resulted in limited success, and currently new forms of curcumin derivatives and nanoformulations are under investigation. In our study, we propose a simple and effective method of curcumin formulation that includes benefits of both new approaches. Nanogel–drug conjugates recently introduced by our laboratory have advantages of drug protection, sustained zero-order kinetics of drug release without initial burst effect, and efficient drug internalization in cancer cells due to the strong cholesteryl–polymer affinity to cellular membrane.[21] Many aggressive and metastatic cancers and cancer stem cells express high level of CD44 receptors, which bind with

hyaluronic acid. It allows for faster spreading and attachment of cancer cells to connective tissue and cartilage. Our design included synthesis of small nanogel particles of CHA-CUR by modification of hyaluronic acid with cholesterol, and then with curcumin via reversible ester bonds. This is the major feature of nanogel–drug conjugates compared to polymer–drug conjugates. The polymeric drugs have often a lower activity than small drug molecules, by evident physicochemical reasons, while nanogel–drug conjugates demonstrate usually much higher therapeutic efficacy. A good illustration of this fact can be the comparison of cancer cytotoxicity of HA–drug conjugates with CHA–drug conjugates.[21] CHA-CUR also induced higher *in vitro* cytotoxicity and apoptosis in cancer cells compared with free drug through the effective inhibition of the same molecular targets as for curcumin, which influence tumor initiation, promotion, angiogenesis, and metastasis.[5] We observed a stronger reduction of mRNA expression of these targets in CHA-CUR group for a longer period, probably due to the sustained release of active curcumin from CHA-CUR compared to fast free curcumin degradation. Thus, CHA-CUR can potentially be used as a cancer-preventing agent or an agent preventing tumor relapse after chemotherapy.

The synthesis of CHA-CUR nanogel was optimized to reduce exposure to harmful organic solvents and reagents.[21] Nanogel backbone was made of HA with Mw 62 kDa, which allowed us to achieve the efficient binding with CD44 receptor
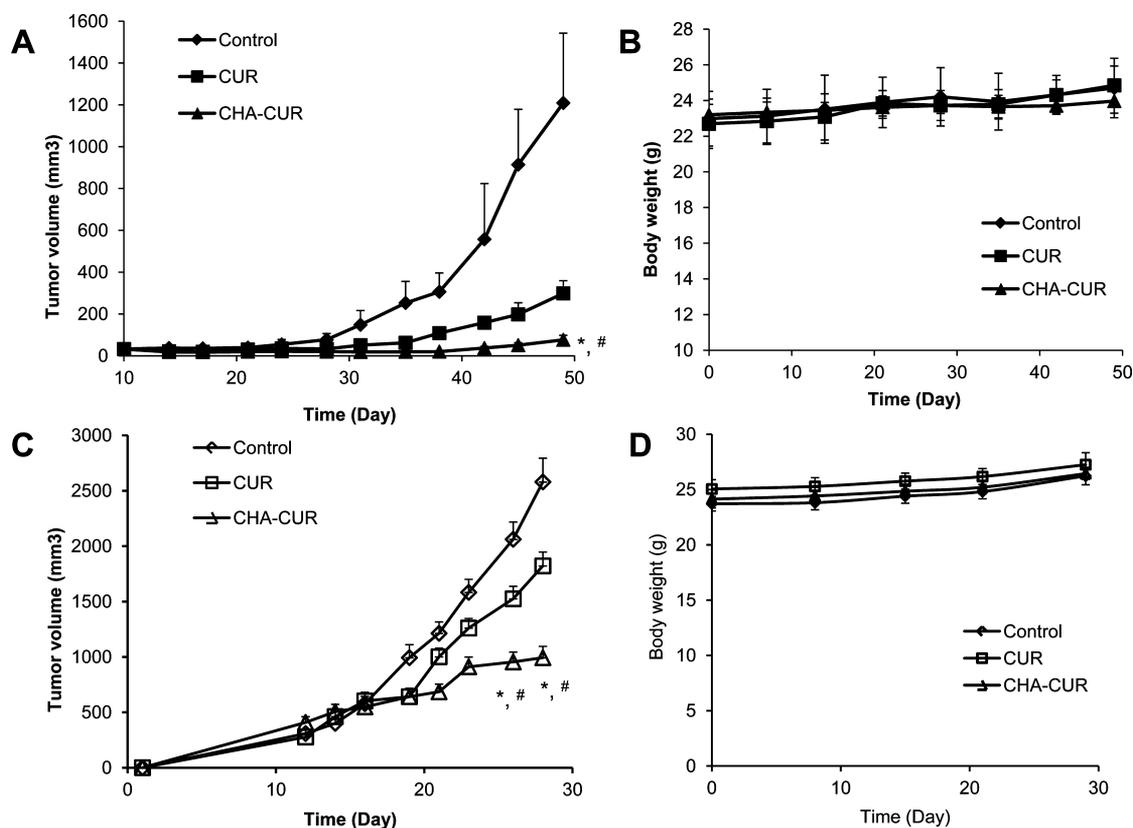
Figure 7. Tumor growth inhibition in animal cancer models after treatments with the nanodrug. (A) In MiaPaCa-2 xenograft model, mice have been treated twice a week by *i.p.* injections of the solution of CHA-CUR in saline or curcumin in DMSO at equal drug doses of 6 mg/kg. (C) In 4T1 orthotropic model, mice were treated by oral gavage with the solution of CHA-CUR in water or curcumin in 70% DMSO at equal drug doses of 12 mg/kg. *, $P < 0.05$, CHA-CUR vs control; #, $P < 0.05$, curcumin vs CHA-CUR. (B,D) Body weight change during the treatment of MiaPaCa-2 and 4T1 animal models, respectively. Data are means ± SEM ($n = 8$).

in cancer cells. It was found that only HA with MW higher than 30 kDa has a good CD44 binding affinity.[26] The number of cholesterol moieties and the curcumin loading in CHA-CUR have been optimized to obtain compact particles and achieve efficient cellular internalization and good solubility. The curcumin loading could be as high as 20% by weight, which is much higher than usual drug content in liposomal or other nanoparticulate carriers.[27] We used CHA-CUR obtained from CHA 1_6 (six cholesteryl molecules per HA) and medium curcumin content (7%) in this study to ensure good nanodrug solubility; for example, CHA 1_18 nanogel showed lower solubility. At 4 °C, when endocytosis was suppressed, we observed a linear increase of the cellular accumulation of CHA nanogels depending on the increase in cholesterol content. Thus, nanogels with the cholesterol content of more than six molecules per HA are taken by cancer cells not only by CD44 receptor-mediated endocytosis but also through direct binding with cellular membrane, evidently due to the cholesterol anchoring in phospholipid bilayer. Uncoiling on the cellular membrane after interaction with cellular receptors allows nanogel–drug conjugates to tightly bind the membrane and fuse with it resulting in the sustained drug release directly into cytoplasm.

The tumor targeting ability and efficient internalization were clearly contributed to the outstanding activity of CHA-CUR. Our uptake study demonstrated that CHA nanogels preferentially target cancer cells through the CD44-mediated clathrin-dependent endocytosis. The tumor accumulation of CHA-CUR was even higher compared with the relevant HA-based

nanoparticles.[28,29] Many nanocarriers are accumulated in RES organs like liver and spleen.[30] Since liver is a major site of HA metabolism and recycle, we also observed accumulation of CHA-CUR in liver. This result was opposite to PEGylated HA nanoparticles, which showed higher accumulation in kidney than in liver.[29]

Stability of nanodrugs in the GI tract is an important factor when the oral administration is considered. Therapeutic efficacy of CHA-CUR depends on curcumin stability and the drug release rate. We found that redox degradation of curcumin in CHA-CUR was less than 10% after 24 h incubation in aqueous solution, while most of the free curcumin completely degraded already in 60 min in the same conditions.[21] Earlier reports suggested that the redox stability of curcumin could be improved by esterification of phenol hydroxyls.[19,31] We observed a slow cleavage of ester bond in CHA-CUR under the GI conditions. Thus, only a small amount of CHA-CUR (2–5%) was lost in the GI tract due to the curcumin release, and the majority of nanodrug was able to enter blood circulation. Exposure to SGF and SIF did not affect significantly the stability of nanodrug.

The size of nanocarriers is important for effective drug delivery. It was reported that nanocarriers with a diameter of 30–50 nm are rapidly transported across mucosa, a fundamental layer in the GI tract.[32] We previously demonstrated that nanogel–drug conjugates of cholesteryl-poly(vinyl alcohol)s (CPVA) of 30–40 nm in diameter are able to efficiently penetrate through an *in vitro* Caco-2 cellular monolayer, as a model of the GI tract.[23] The permeability of
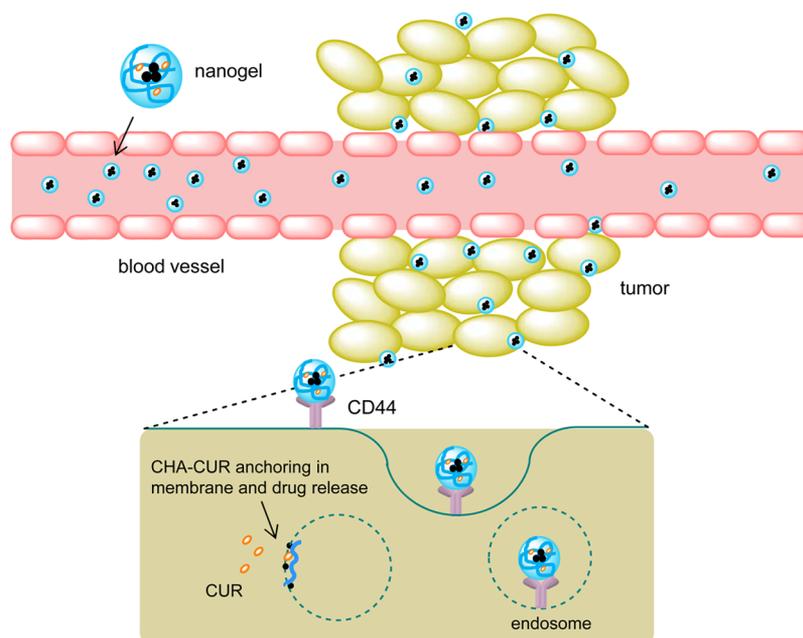
Figure 8. Illustration of the targeted nanogel delivery to cancer cells. CHA-CUR circulated in blood and accumulated in tumor via leaky tumor neovasculature (EPR effect). It targeted cancer cells in metastases through CD44-binding and penetrated them via receptor-mediated endocytosis. Anchoring and fusion of nanogels with cellular membrane facilitated sustained release of active curcumin in cytosol through hydrolysis of ester bonds in CHA-CUR.

CHA−drug conjugates in the same model system was medium (permeability coefficient, P_{app}, 1.18×10^{-6} cm^{-1}). Drugs with a P_{app} between 10^{-6} and 10^{-5} regularly have 20−70% GI permeability *in vivo*.[23] After absorption in the GI tract, CHA-CUR can enter the bloodstream and be delivered to CD44-expressing tumors. The particle size also affects the capture of nanodrugs by peripheral macrophages from blood circulation. It was found that nanoparticle with the size below 200 nm are captured less efficiently by RES macrophages.[33] CHA-CUR has a hydrodynamic diameter of 20s nm, which is in the optimal range for anticancer therapeutic applications.

CHA-CUR demonstrated advanced pharmacokinetic parameters compared to free curcumin. Anticancer efficacy of curcumin was limited by its poor bioavailability. Poor solubility of curcumin resulted in low GI absorption, while the instability of curcumin in blood shortened its therapeutic window. Earlier studies showed very low-to-undetectable curcumin levels in plasma already 1 h after *i.p.* administration, irrespective of the administrated doses.[14,34] Compared with curcumin or liposomal curcumin, CHA-CUR showed elevated AUC, longer circulation time, and slower clearance from the body.[24,25] The improved PK profile of CHA-CUR suggests it should have a potent therapeutic effect *in vivo*. Orally administered CHA-CUR also showed very satisfactory PK profile, confirming the efficacy of oral administration of this nanodrug.

Figure 8 illustrates three major steps of the nanotherapy. From the blood, CHA-CUR can bind CD44-expressing metastases and accumulate in tumors via the enhanced permeability and retention (EPR) effect. Then, it is efficiently internalized in cancer cells and releases curcumin in sustained mode inside cancer cells, resulting in apoptosis and tumor growth inhibition.

Our tumor growth inhibition studies in animal tumor models produced very promising results on the therapeutic effect of CHA-CUR at quite low doses. The tumor growth was fast in the control group and practically uninhibited in curcumin-treated group. CHA-CUR-treated mice displayed statistically significant suppression of tumor growth even at relatively low doses of nanodrug. Low toxicity and high solubility of the CHA-CUR allowed substantial increase in administered dose. High antitumor activity of CHA-CUR is related primarily to its good bioavailability, accumulation in cancer cells, and drug stability during the therapy, while the administered curcumin lacked all these advantages. Intraperitoneal and oral administration of CHA-CUR both showed potent antitumor efficacy. Thus, oral CHA-CUR, as the most preferable route of administration with excellent pharmacokinetic profile and potent anticancer efficacy *in vivo*, can be recommended as potential novel therapeutic agent for the treatment of aggressive and metastatic cancers.[35]

■ CONCLUSIONS

We demonstrated therapeutic advantages of the nanogel−drug conjugate CHA-CUR compared to free drug in effective cancer therapy. The new nanodrug showed excellent aqueous solubility, stability, bioavailability, and therapeutic efficacy due to the tumor-targeted delivery, efficient accumulation in cancer cells, and sustained release of active drug. It was active against the same cellular targets as curcumin and demonstrated increased apoptosis and cytotoxicity compared to curcumin against different cancer cells. CHA-CUR showed prolonged circulation in blood compared to curcumin, efficiently accumulated in tumors *in vivo*, and was active in both xenograft and orthotropic tumor animal models at *i.p.* and oral administrations. Thus, this simple, very effective and nontoxic nanodrug exhibits high potential as new anticancer drug type with therapeutic and preventive applications.

■ ASSOCIATED CONTENT

S **Supporting Information**

Scheme of the synthesis of CHA-CUR, ^{1}H NMR spectra, DLS analysis, and TEM images of CHA-CUR, and other characterization data. This material is available free of charge via the Internet at http://pubs.acs.org.

■ AUTHOR INFORMATION

Corresponding Author

*(S.V.V.) Address: 986025 Nebraska Medical Center, Omaha, Nebraska 68198-6025, United States. Phone: +1 (402) 559-9362. Fax: +1(402) 559-9543. E-mail: vinograd@unmc.edu.

Notes

The authors declare no competing financial interest.

■ ACKNOWLEDGMENTS

■ REFERENCES

(1) Johnson, J. J.; Mukhtar, H. Curcumin for chemoprevention of colon cancer. *Cancer Lett.* **2007**, 255 (2), 170−81.

(2) Liu, D.; Chen, Z. The effect of curcumin on breast cancer cells. *J. Breast Cancer* **2013**, 16 (2), 133−7.

(3) Chen, H. W.; Lee, J. Y.; Huang, J. Y.; Wang, C. C.; Chen, W. J.; Su, S. F.; Huang, C. W.; Ho, C. C.; Chen, J. J.; Tsai, M. F.; Yu, S. L.; Yang, P. C. Curcumin inhibits lung cancer cell invasion and metastasis through the tumor suppressor HLJ1. *Cancer Res.* **2008**, 68 (18), 7428−38.

(4) Jutooru, I.; Chadalapaka, G.; Lei, P.; Safe, S. Inhibition of NFkappaB and pancreatic cancer cell and tumor growth by curcumin is dependent on specificity protein down-regulation. *J. Biol. Chem.* **2010**, 285 (33), 25332−44.

(5) Joe, B.; Vijaykumar, M.; Lokesh, B. R. Biological properties of curcumin-cellular and molecular mechanisms of action. *Crit Rev. Food Sci. Nutr.* **2004**, 44 (2), 97−111.

(6) Choi, B. H.; Kim, C. G.; Lim, Y.; Shin, S. Y.; Lee, Y. H. Curcumin down-regulates the multidrug-resistance mdr1b gene by inhibiting the PI3K/Akt/NF kappa B pathway. *Cancer Lett.* **2008**, 259 (1), 111−8.

(7) Aggarwal, B. B.; Shishodia, S.; Takada, Y.; Banerjee, S.; Newman, R. A.; Bueso-Ramos, C. E.; Price, J. E. Curcumin suppresses the paclitaxel-induced nuclear factor-kappaB pathway in breast cancer cells and inhibits lung metastasis of human breast cancer in nude mice. *Clin. Cancer Res.* **2005**, 11 (20), 7490−8.

(8) Shakibaei, M.; Mobasheri, A.; Lueders, C.; Busch, F.; Shayan, P.; Goel, A. Curcumin enhances the effect of chemotherapy against colorectal cancer cells by inhibition of NF-kappaB and Src protein kinase signaling pathways. *PLoS One* **2013**, 8 (2), e57218.

(9) Liu, Q.; Loo, W. T.; Sze, S. C.; Tong, Y. Curcumin inhibits cell proliferation of MDA-MB-231 and BT-483 breast cancer cells mediated by down-regulation of NFkappaB, cyclinD and MMP-1 transcription. *Phytomedicine* **2009**, 16 (10), 916−22.

(10) Haefner, B. NF-kappa B: arresting a major culprit in cancer. *Drug Discovery Today* **2002**, 7 (12), 653−63.

(11) Goel, A.; Boland, C. R.; Chauhan, D. P. Specific inhibition of cyclooxygenase-2 (COX-2) expression by dietary curcumin in HT-29 human colon cancer cells. *Cancer Lett.* **2001**, 172 (2), 111−8.

(12) Kunnumakkara, A. B.; Guha, S.; Krishnan, S.; Diagaradjane, P.; Gelovani, J.; Aggarwal, B. B. Curcumin potentiates antitumor activity of gemcitabine in an orthotopic model of pancreatic cancer through suppression of proliferation, angiogenesis, and inhibition of nuclear factor-kappaB-regulated gene products. *Cancer Res.* **2007**, 67 (8), 3853−61.

(13) Shishodia, S.; Chaturvedi, M. M.; Aggarwal, B. B. Role of curcumin in cancer therapy. *Curr. Probl. Cancer* **2007**, 31 (4), 243−305.

(14) Anand, P.; Kunnumakkara, A. B.; Newman, R. A.; Aggarwal, B. B. Bioavailability of curcumin: problems and promises. *Mol. Pharmaceutics* **2007**, 4 (6), 807−18.

(15) Anand, P.; Nair, H. B.; Sung, B.; Kunnumakkara, A. B.; Yadav, V. R.; Tekmal, R. R.; Aggarwal, B. B. Design of curcumin-loaded PLGA nanoparticles formulation with enhanced cellular uptake, and increased bioactivity in vitro and superior bioavailability in vivo. *Biochem. Pharmacol.* **2010**, 79 (3), 330−8.

(16) Chen, C.; Johnston, T. D.; Jeon, H.; Gedaly, R.; McHugh, P. P.; Burke, T. G.; Ranjan, D. An in vitro study of liposomal curcumin: stability, toxicity and biological activity in human lymphocytes and Epstein-Barr virus-transformed human B-cells. *Int. J. Pharm.* **2009**, 366 (1−2), 133−9.

(17) Li, J.; Wang, Y.; Yang, C.; Wang, P.; Oelschlager, D. K.; Zheng, Y.; Tian, D. A.; Grizzle, W. E.; Buchsbaum, D. J.; Wan, M. Polyethylene glycosylated curcumin conjugate inhibits pancreatic cancer cell growth through inactivation of Jab1. *Mol. Pharmacol.* **2009**, 76 (1), 81−90.

(18) Yallapu, M. M.; Othman, S. F.; Curtis, E. T.; Bauer, N. A.; Chauhan, N.; Kumar, D.; Jaggi, M.; Chauhan, S. C. Curcumin-loaded magnetic nanoparticles for breast cancer therapeutics and imaging applications. *Int. J. Nanomed.* **2012**, 7, 1761−79.

(19) Yang, R.; Zhang, S.; Kong, D.; Gao, X.; Zhao, Y.; Wang, Z. Biodegradable polymer-curcumin conjugate micelles enhance the loading and delivery of low-potency curcumin. *Pharm. Res.* **2012**, 29 (12), 3512−25.

(20) Manju, S.; Sreenivasan, K. Conjugation of curcumin onto hyaluronic acid enhances its aqueous solubility and stability. *J. Colloid Interface Sci.* **2011**, 359 (1), 318−25.

(21) Wei, X.; Senanayake, T. H.; Warren, G.; Vinogradov, S. V. Hyaluronic acid-based nanogel-drug conjugates with enhanced anticancer activity designed for the targeting of CD44-positive and drug-resistant tumors. *Bioconjugate Chem.* **2013**, 24 (4), 658−68.

(22) Lacerda, L.; Russier, J.; Pastorin, G.; Herrero, M. A.; Venturelli, E.; Dumortier, H.; Al-Jamal, K. T.; Prato, M.; Kostarelos, K.; Bianco, A. Translocation mechanisms of chemically functionalised carbon nanotubes across plasma membranes. *Biomaterials* **2012**, 33 (11), 3334−43.

(23) Senanayake, T. H.; Warren, G.; Wei, X.; Vinogradov, S. V. Application of activated nucleoside analogs for the treatment of drug-resistant tumors by oral delivery of nanogel-drug conjugates. *J. Controlled Release* **2013**, 167 (2), 200−9.

(24) Yang, K. Y.; Lin, L. C.; Tseng, T. Y.; Wang, S. C.; Tsai, T. H. Oral bioavailability of curcumin in rat and the herbal analysis from Curcuma longa by LC-MS/MS. *J. Chromatogr. B: Anal. Technol. Biomed. Life Sci.* **2007**, 853 (1−2), 183−9.

(25) Li, J.; Jiang, Y.; Wen, J.; Fan, G.; Wu, Y.; Zhang, C. A rapid and simple HPLC method for the determination of curcumin in rat plasma: assay development, validation and application to a pharmacokinetic study of curcumin liposome. *Biomed. Chromatogr.* **2009**, 23 (11), 1201−7.

(26) Wolny, P. M.; Banerji, S.; Gounou, C.; Brisson, A. R.; Day, A. J.; Jackson, D. G.; Richter, R. P. Analysis of CD44-hyaluronan interactions in an artificial membrane system: insights into the distinct binding properties of high and low molecular weight hyaluronan. *J. Biol. Chem.* **2010**, 285 (39), 30170−80.

(27) Vinogradov, S. V.; Kohli, E.; Zeman, A.; Kabanov, A. V. Chemical engineering of nanogel drug carriers: increased bioavailability and decreased cytotoxicity. *Polym. Prepr.* **2006**, 47 (2), 27−28.

(28) Cho, H. J.; Yoon, H. Y.; Koo, H.; Ko, S. H.; Shim, J. S.; Lee, J. H.; Kim, K.; Kwon, I. C.; Kim, D. D. Self-assembled nanoparticles based on hyaluronic acid-ceramide (HA-CE) and pluronic(R) for tumor-targeted delivery of docetaxel. *Biomaterials* **2011**, 32 (29), 7181−90.

(29) Cho, H. J.; Yoon, I. S.; Yoon, H. Y.; Koo, H.; Jin, Y. J.; Ko, S. H.; Shim, J. S.; Kim, K.; Kwon, I. C.; Kim, D. D. Polyethylene glycol-conjugated hyaluronic acid-ceramide self-assembled nanoparticles for targeted delivery of doxorubicin. *Biomaterials* **2012**, *33* (4), 1190−200.

(30) Lankveld, D. P.; Oomen, A. G.; Krystek, P.; Neigh, A.; Troost-de Jong, A.; Noorlander, C. W.; Van Eijkeren, J. C.; Geertsma, R. E.; De Jong, W. H. The kinetics of the tissue distribution of silver nanoparticles of different sizes. *Biomaterials* **2010**, *31* (32), 8350−61.

(31) Wichitnithad, W.; Nimmannit, U.; Callery, P. S.; Rojsitthisak, P. Effects of different carboxylic ester spacers on chemical stability, release characteristics, and anticancer activity of mono-PEGylated curcumin conjugates. *J. Pharm. Sci.* **2011**, *100* (12), 5206−18.

(32) Ghosn, B.; van de Ven, A. L.; Tam, J.; Gillenwater, A.; Sokolov, K. V.; Richards-Kortum, R.; Roy, K. Efficient mucosal delivery of optical contrast agents using imidazole-modified chitosan. *J. Biomed. Opt.* **2010**, *15* (1), 015003.

(33) Yuan, F.; Dellian, M.; Fukumura, D.; Leunig, M.; Berk, D. A.; Torchilin, V. P.; Jain, R. K. Vascular permeability in a human tumor xenograft: molecular size dependence and cutoff size. *Cancer Res.* **1995**, *55* (17), 3752−6.

(34) Bisht, S.; Mizuma, M.; Feldmann, G.; Ottenhof, N. A.; Hong, S. M.; Pramanik, D.; Chenna, V.; Karikari, C.; Sharma, R.; Goggins, M. G.; Rudek, M. A.; Ravi, R.; Maitra, A. Systemic administration of polymeric nanoparticle-encapsulated curcumin (NanoCurc) blocks tumor growth and metastases in preclinical models of pancreatic cancer. *Mol. Cancer Ther.* **2010**, *9* (8), 2255−64.

(35) Vinogradov, S. V.; Senanayake, T. Nanogel-drug conjugates: a step towards increasing the chemotherapeutic efficacy. *Nanomedicine (London, U. K.)* **2013**, *8* (8), 1229−1232.